Applied Radiation and Isotopes 69 (2011) 1870–1873

Contents lists available at ScienceDirect

Applied Radiation and Isotopes

journal homepage: www.elsevier.com/locate/apradiso

Treatment planning capability assessment of a beam shaping assembly for accelerator-based BNCT

M.S. Herrera [a,b,c,*], S.J. González [a,b], A.A. Burlon [a,c], D.M. Minsky [a,b,c], A.J. Kreiner [a,b,c]

[a] Comisión Nacional de Energía Atómica, CNEA, Av. Gral. Paz 1499, San Martín, Argentina
[b] Consejo Nacional de Investigaciones Científicas y Técnicas, CONICET, Av. Rivadavia 191, Buenos Aires, Argentina
[c] Universidad Nacional de San Martín, UNSAM, Av. 25 de Mayo y Francia Buenos Aires, Argentina

ARTICLE INFO

Article history:
Received 9 December 2010
Received in revised form
4 March 2011
Accepted 17 March 2011
Available online 7 April 2011

Keywords:
Accelerator-based BNCT
Beam shaping assembly
Treatment planning

ABSTRACT

Within the frame of an ongoing project to develop a folded Tandem-Electrostatic-Quadrupole accelerator facility for Accelerator-Based Boron Neutron Capture Therapy (AB-BNCT) a theoretical study was performed to assess the treatment planning capability of different configurations of an optimized beam shaping assembly for such a facility. In particular this study aims at evaluating treatment plans for a clinical case of Glioblastoma.

1. Introduction

An ongoing project to develop a folded Tandem-Electrostatic-Quadrupole accelerator-based BNCT facility is being designed and constructed at CNEA's atomic center Constituyentes in Buenos Aires, Argentina. The machine under development takes advantage of the ^{7}Li(n,p)^{7}Be reaction to generate a neutron beam from the primary proton flux. The neutron spectrum obtained must be optimized with a beam shaping assembly before it can be used for clinical purposes. In this context, different optimized neutron beam shaping assemblies for such a facility have been studied and proposed by Burlon et al. (2004, 2005) and Minsky et al. (2010). In those studies the optimization was made by evaluating the doses delivered to the Snyder head phantom model and taking into account the treatment time. Dose assessment was performed through the calculation of a tumor control probability proposed by Laramore et al. (1996). At this point, subtle differences between designs must be evaluated using Monte Carlo simulations in treatment planning for real patients. In this paper, the treatment planning capability of three beam shaping assemblies was compared.

2. Materials and methods

2.1. Treatment planning

Due to the fact that the accelerator-based BNCT considered in this work may supply an epithermal neutron beam, the case of a real patient with glioblastoma multiforme was considered. Based on the tagged CT images of the patient, both the volume and the position of the tumor inside the head were computed. The tumor spheroid, with 2 cm for its largest diameter, was located at 3 cm depth in the occipital lobe of the brain. The CT stack also allowed to voxelize the patient head using the NCTPlan treatment code (González et al., 2002), for the simulated irradiation. The neutron beam direction in the simulation was determined based on the location of the lesion and using the NCTPlan in order to deliver the maximum dose to the tumor but, for simplicity, only one field was modeled.

Both maximum and mean normal brain doses have been used in most protocols as the prescription dose. In this work, a peak dose of 11 Gy-Eq to the normal brain was adopted as the prescription dose and a volume average brain dose of 7 Gy-Eq was considered. Regarding the skin, a conservative upper limit of 16.7 Gy-Eq was used. In this work we have only studied the dose in the patient / head phantom. The whole body dose will be calculated for all configurations in future work.

2.2. Simulations

For dose Monte Carlo calculations, the theoretical neutron source from Lee and Zhou (1999) for the ^{7}Li(n,p)^{7}Be reaction at

* Corresponding author at: Comisión Nacional de Energía Atómica, CNEA, Av. Gral. Paz 1499, San Martín, Argentina. Tel.: +54 11 6772 7103.
E-mail address: herrera@tandar.cnea.gov.ar (M.S. Herrera).

0969-8043/$ - see front matter © 2011 Elsevier Ltd. All rights reserved.
doi:10.1016/j.apradiso.2011.03.029

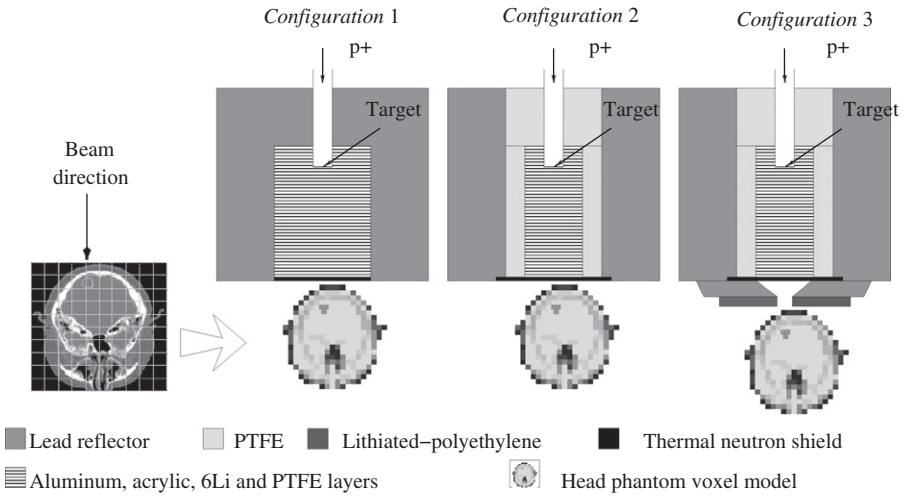

Fig. 1. Representation of the beam shaping assemblies considered in this work. The square beam aperture sizes are: 25 cm × 25 cm and 15 cm × 15 cm for Configuration 1 and 2, respectively. Configuration 3 is identical to 2 but includes a funnel type collimator.

Table 1
Tumor to blood and normal tissue to blood ^{10}B concentration ratios, relative biological effectiveness (RBE) and compound relative biological effectiveness (CBE) factors for each dose component and tissue used for dose calculation.

Tissue	RBE		CBE	Ratio
	Gamma	Thermal/fast neutron	Boron (BPA)	
Brain	1	3.2	1.3	1
Skin	1	3.2	2.5	1.5
Tumor	1	3.2	3.8	3.5

2.3 and 2.6 MeV was used, assuming a 30 mA current proton beam and a metallic Li or a LiF target. The neutron transport starts at the target, going through the moderator and up to the patient phantom head. The phantom is divided into 1 cm^3 voxels in a 21 × 21 × 25 lattice (see Fig. 1) where the physical dose rate was computed via MCNP5 (LANL, 2003) taking into account the proper Kerma factors. Typical runs involved 10^9 particles yielding relative statistical errors between 5–10%. Finally to compute the total weighted dose, the tissue to blood and tumor to blood ^{10}B concentration ratios, the relative biological effectiveness and the compound relative biological effectiveness factors were used (Table 1). This procedure was followed in three cases where different moderator–reflector or beam shaping assemblies (BSAs) were considered.

2.3. Beam shaping assembly designs

The neutron source produced by protons on the target has to be moderated to obtain the desired epithermal neutron beam centered at approximately 10 keV. Different combinations of thick layers of materials such as aluminum, acrylic, ^6Li and polytetrafluoroethylene (PTFE) have been used to moderate the neutrons. Also lead was employed as a neutron reflector and a 5 mm layer of enriched $^6Li_2CO_3$ (95%) was used to filter out the thermal neutrons, reducing the absorbed skin dose in the head. Fig. 1 shows the three BSAs considered in this work. The main geometrical difference between designs is the beam aperture or exit port size. Configuration 1 and 2 exhibit a square exit port size of 25 cm × 25 cm and 15 cm × 15 cm, respectively, defined as the entire area between the lead reflector blocks. Configuration 3, which is identical to Configuration 2, includes also a funnel type collimator made of 50 mm of lead and 20 mm of lithiated-polyethilene.

In the optimization process of Configuration 1, several parameters were varied. In particular, proton beam energies from 2.0 to 2.8 MeV have been explored. According to those results, a 2.6 MeV proton beam energy was employed for this configuration, while for both Configuration 2 and 3 a closer value to the $^7Li(p,n)^7Be$ resonance at 2.3 MeV were used. The metallic Li target and the LiF target were considered for dose calculation in all cases.

2.4. Assessment

The evaluation of the results obtained from the simulations for the regions of interest (tumor, normal brain and skin) was made using several figures of merit. As a first step the irradiation time and the maximum, mean and minimum doses for tumor and healthy tissue were computed and compared. Based on the depth-dose profiles along the beam direction through the brain, the advantage depth was calculated. In order to take into account the 3D dose distribution for brain and tumor, dose–volume histograms were plotted and the dose inhomogeneity was compared. Finally, regarding the skin, cumulative dose-area histograms and a related figure of merit, the normal tissue complication probability, were computed for each configuration to take into account the possible early skin effects.

3. Results and discussion

As mentioned in the Treatment planning section, the results obtained from the simulations were assessed setting the maximum tolerable dose to normal brain to 11 Gy-Eq and, at the same time, it was verified that the mean dose to the whole-brain (both hemispheres) did not exceed 7 Gy-Eq. In Fig. 2 the total dose rate profiles along the beam direction through the head for Configuration 2 are shown. The figure also plots each individual component according to the kind of tissue for that depth (i.e. normal skin at 0 cm and normal brain starting from 1 cm) weighted with the radiobiological factors given in Table 1. The total dose for tumor and brain along the beam direction obtained for Configuration 2 after 18 min of irradiation (considering the metallic Li target) is shown in Fig. 3. The derived advantage depth (AD) of 10.7 cm is also shown.

A similar analysis was made for Configuration 1 and 3. The total irradiation time in these cases was 10 and 54.6 min

respectively for the Li metal target. As for the LiF option, the treatment times are tripled to obtain an identical dosimetry. The derived advantage depths of 10.8 and 10.7 cm were found for Configuration 1 and 3, respectively. It is worth pointing out that the three assessed configurations exhibited similar maximum dose rate at ~3 cm depth.

Table 2 shows the maximum, mean and minimum doses for brain and tumor for Configuration 1, 2 and 3. Considering the statistical errors of the calculations, there are no significant differences between different configurations for each parameter of interest in the tumor and for the normal brain, the three configurations provided the same average brain dose around 5 Gy-Eq. Despite the fact that increasing the number of particles in the run, statistical errors may be low enough to reveal differences between the dose values, from a clinical point of view those differences are unimportant compared with other uncertainties in BNCT (such as boron distribution).

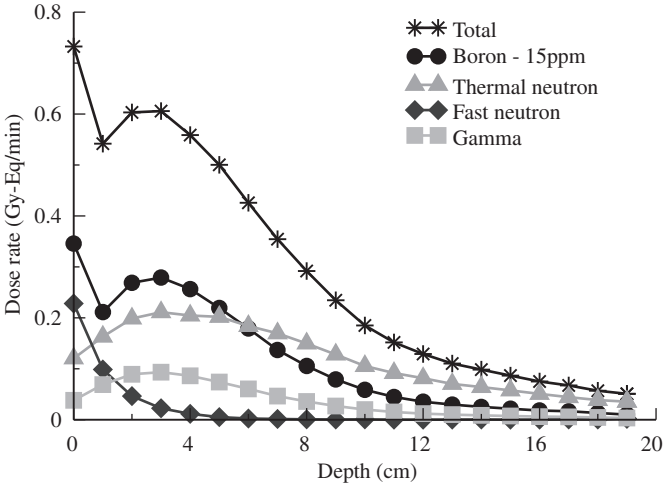

Fig. 2. Profiles of the biologically-weighted absorbed-dose rate components along the beam direction for Configuration 2, considering 15 ppm of ^{10}B concentration in blood.

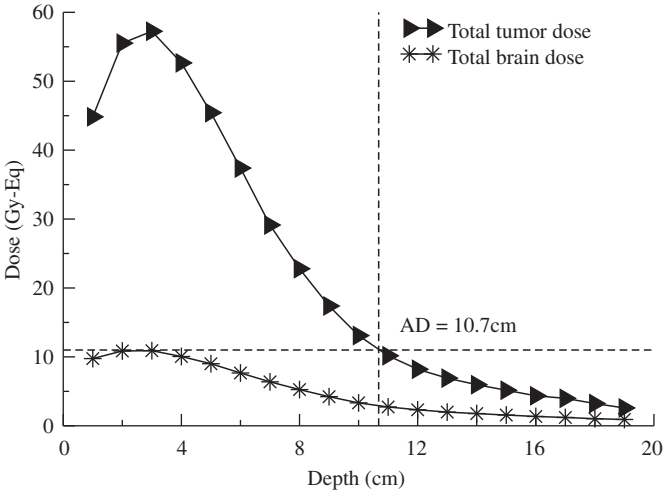

Fig. 3. Depth-dose profile along the beam direction for brain and tumor after 18 minutes irradiation (considering 15 ppm of ^{10}B concentration) for Configuration 2. The derived advantage depth (AD) is shown.

The estimation of the brain tolerance dose made from the Brookhaven and Harvard-MIT patient data set (Coderre et al., 2004; Riley et al., 2008) indicates that the development of somnolence (as evaluated endpoint) in some patients occurs when the brain receives a peak dose above 11 Gy-Eq and simultaneously, the whole-brain average is between 5 and 7 Gy-Eq. Furthermore, all patients receiving above 7 Gy-Eq developed somnolence. The AB-BNCT results obtained for the present case considering the prescription dose to the normal brain of 11 Gy-Eq, show that the whole-brain average dose does not exceed (5.0 ± 0.5)Gy-Eq for all BSA configurations used in the simulations. It should be mentioned that only one field was analyzed in this work. In the future, it will be necessary to study the effect of multiple fields in the mean value and peak dose derived from the configurations presented herein.

It is possible to acquire more information to evaluate differences between designs if dose–volume histograms (DVHs) are studied for healthy tissue and tumor. Fig. 4 shows the DVHs for both brain and tumor separately by regions.

In region I of Fig. 4, the DVH for brain (1298.5 cm^3) shows no differences between Configuration 1, 2 and 3. On the other hand, region II exhibits the dose in the tumor (4.2 cm^3) where higher doses are delivered. Tumor dose values between configurations agree within statistical uncertainties. However, as a measure of the spatial inhomogeneity, the difference between the tumor doses $D_{95\%}$ and $D_{5\%}$ was computed. Taking into account such parameter Configuration 3 presents a greater spatial inhomogeneity than Configuration 1 and 2, the difference being about 30%. It is also possible to compute the dose-area histogram (DAH) for skin by considering the most superficial layer (Fig. 4, bottom right). Maximum skin doses below the tolerable dose considered in this paper, of 12.5, 11.5 and 15 Gy-Eq for Configuration 1, 2 and 3, respectively, were found. However the irradiated areas are quite different because of the size of the beam ports.

Normal tissue complication probability (NTCP) for inhomogeneous dose distributions was previously studied by González et al. (2009) in BNCT treatments of nodular melanoma. Following the lines and the formalism of the equivalent sub-volume model, it was found that Configuration 1, 2 and 3 derive a 72%, 35% and 42% probability to cause skin moist desquamation in the patient's head, respectively. The NTCP values obtained show that the reduction in the area of irradiation in Configuration 3 via the collimator would not represent a better irradiation in terms of possible damage to the skin. Although the high-dose irradiated skin area was substantially smaller for this case, the important increase in the maximum skin dose eventually raised the NCTP value up.

Table 2
Maximum, mean and minimum doses for brain and tumor obtained after 10, 18 and 54.6 min and 15 ppm of ^{10}B concentration in blood for the metallic Li target option for Configuration 1, 2 and 3, respectively. The prescription dose* considered in this work was 11 Gy-Eq for normal brain. Relative statistical errors are between 5 and 10%.

Dose (Gy-Eq)	Tumor			Normal brain		
	Configuration 1	Configuration 2	Configuration 3	Configuration 1	Configuration 2	Configuration 3
Maximum	55	57	52	11.0*	11.0*	11.0*
Mean	52	54	48	5.0	5.0	4.7
Minimum	47	48	42	1.0	0.6	2.0

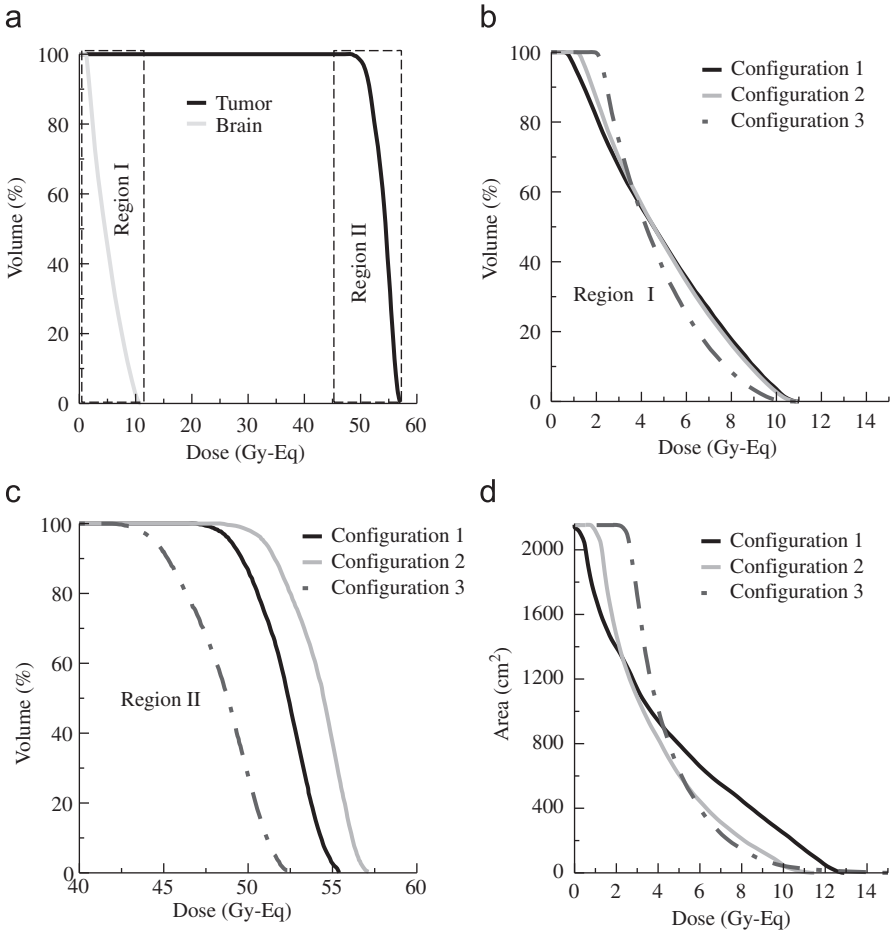

Fig. 4. Dose–volume histograms (DVHs) for brain (excluding the tumor) and tumor and dose-area histogram (DAH) for skin are shown for each configuration.

4. Conclusion

Based on dose prescriptions, all the studied configurations lead to high equivalent tumor doses. It was found that the figures of merit regarding treatment time, homogeneity and NTCP are the main quantities distinguishing between the three schemes in favor of Configuration 2. The results also suggest that for a full characterization of optimal configurations in AB-BNCT, some radiobiological figures of merit should be considered. As it was shown in this work in the case of the NTCP for the skin, such figures may exhibit important differences depending on the geometry and size of the beam port.

Acknowledgments

This work was partially supported by CONICET and ANPCyT.

References

Burlon, A.A., et al., 2004. An optimized neutron-beam shaping assembly for accelerator-based BNCT. Appl. Radiat. Isot. 61, 811–815.

Burlon, A.A., et al., 2005. Optimization of a neutron production target and a beam shaping assembly based on the ^{7}Li(n,p)^{7}Be reaction for BNCT. Nucl. Instrum. Methods B 229, 144–156.

Coderre, J.A., et al., 2004. Tolerance of normal human brain to boron neutron capture therapy. Appl. Radiat. Isot. 61, 1083–1087.

González, S.J., et al., 2009. Tumor control and normal tissue complications in BNCT treatment of nodular melanoma: a search for predictive quantities. Appl. Radiat. Isot. 67, 153–156.

González, S.J., et al., 2002. NCTPlan, the new PC version of MacNCTPlan: improvements and verification of a BNCT treatment planning system. In: Sauerwein, W., Moss, R., Wittig, A. (Eds.), Proceedings of the 10th International Congress on Neutron Capture Therapy for Cancer. Monduzzi Editore, Germany, pp. 557–561.

LANL, 2003. A General Monte Carlo N Particle Transport Code, version 5, LA-UR-03-1987.

Laramore, G.E., et al., 1996. A BNCT tumor control curve for malignant glioma from fast neutron radiotherapy data: implications for beam delivery and compound selection. In: Larsson, B., Crawford, J., Weinreich, R. (Eds.), Proceedings of the 17th International Symposium on Neutron Capture for Cancer. Elsevier Science, Amsterdam.

Lee, C.L., Zhou, X.L., 1999. Thick target neutron yields for the ^{7}Li(p,n)^{7}Be reaction near threshold. Nucl. Instrum. Methods B 152, 1–11.

Minsky, D.M., et al., 2010. AB-BNCT Beam shaping assembly based on ^{7}Li(p,n)^{7}Be reaction optimization. In: Liberman, S., et al.(Ed.), Proceedings of the 14th International Congress on Neutron Capture Therapy. Comisión Nacional de Energía Atómica, Argentina, pp. 473–479.

Riley, K.J., et al., 2008. An international dosimetry exchange for BNCT Part II: Computational dosimetry normalizations. Med. Phys. 35 (12), 5419–5425.